2002

Direct Electrodeposition of Polypyrrole on Aluminum and Aluminum Alloy by Electron Transfer Mediation

D. E. Tallman
North Dakota State University, USA

C. Vang
North Dakota State University, USA

G G. Wallace
University of Wollongong, gwallace@uow.edu.au

G. P. Bierwagen
North Dakota State University, USA

Journal of The Electrochemical Society, **149** (3) C173-C179 (2002)
0013-4651/2002/149(3)/C173/7/$7.00 © The Electrochemical Society, Inc.

Direct Electrodeposition of Polypyrrole on Aluminum and Aluminum Alloy by Electron Transfer Mediation

D. E. Tallman,[a,*,z] C. Vang,[b,] G. G. Wallace,[c] and G. P. Bierwagen[b,*]**

[a]*Department of Chemistry,* [b]*Department of Polymers and Coatings, North Dakota State University, Fargo, North Dakota 58105-5516, USA*
[c]*Intelligent Polymer Research Institute, University of Wollongong, Wollongong, NSW 2522, Australia*

The direct electrodeposition of electroactive conducting polymers on active metals such as iron and aluminum is complicated by the concomitant metal oxidation that occurs at the positive potentials required for polymer formation. In the case of aluminum and its alloys, the oxide layer that forms is an insulator that blocks electron transfer and impedes polymer formation and deposition. As a result, only patchy nonuniform polymer films are obtained. Electron transfer mediation is a well-known technique for overcoming kinetic limitations of electron transfer at metal electrodes. In this work, we report the use of electron transfer mediation for the direct electrodeposition of polypyrrole onto aluminum and onto Al 2024-T3 alloy. This report focuses on the use of Tiron (4,5-dihydroxy-1,3-benzenedisulfonic acid disodium salt) as the mediator, although catechol appears to function in a similar manner. Depositions were carried out under galvanostatic conditions at current densities of 1 mA/cm^2. The mediator reduced the deposition potential by nearly 500 mV compared to deposition performed in the absence of mediator (where Tiron was replaced by *p*-toluene sulfonic acid sodium salt). Polypyrrole formation and deposition appears to occur with 100% current efficiency and uniform films are obtained. Results of the characterization of these films by scanning electron microscopy, atomic force microscopy, X-ray photoelectron spectroscopy, conductivity measurements, and adhesion measurements are presented.
 [DOI: 10.1149/1.1448820]

Manuscript received July 24, 2001. Available electronically February 7, 2002.

Electroactive conducting polymers (ECPs) are conjugated polymers that exhibit electronic conduction when partially oxidized or reduced (corresponding to p-doped or n-doped polymer, respectively) and are capable of undergoing oxidation/reduction reactions. Examples of ECPs include polyaniline, polypyrrole, polythiophene, and polyphenylenevinylene. These polymers continue to be of considerable research interest and are being explored for a variety of applications, including sensors, actuators, separation membranes, photochromic and photovoltaic devices, and corrosion control coatings.[1,2] ECPs can be synthesized from the appropriate monomers by either chemical or electrochemical polymerization. Electrochemical polymerization is most often carried out at noble metal electrodes such as gold or platinum or sometimes at carbon electrodes.[1] The direct electrochemical polymerization of ECPs at active metal electrodes such as steel or aluminum is complicated by the concomitant oxidation (corrosion) of the metal at the positive potentials required for polymerization. In the case of aluminum, an electrically insulating oxide layer forms that blocks electron transfer and impedes polymer formation and deposition. As a result, only patchy nonuniform polymer films have heretofore been obtained.

Our laboratory has been investigating various ECPs for use as corrosion control coatings.[3-7] Because of the difficulty (described above) in using direct electrodeposition on active metals, the ECP coatings are typically formed by dissolving an appropriately derivatized ECP in an organic solvent and casting the film from the ECP solution. This solvent casting approach works reasonably well, but adhesion, cohesion, and molecular weight of deposited polymer are somewhat limited by this approach. For these reasons, the direct deposition of ECPs on active metals is being explored in our laboratory.

The electrodeposition of ECPs on active metals was pioneered by Beck and co-workers.[8-12] Much of this work focused on electrodeposition of polypyrrole on iron and aluminum from aqueous and nonaqueous electrolytes.[10] For example, electrodeposition of polypyrrole on iron at a current density of 2 mA/cm^2 from aqueous solutions of pyrrole and oxalic acid yielded adherent, smooth polymer films.[11] Active dissolution of the iron was suggested to occur along with formation of an iron(II) oxalate interlayer. Polypyrrole could be deposited on nearly pure aluminum metal (99.5%) from nonaqueous solvents (acetonitrile and methanol) containing small amounts of water and certain organic electrolytes [*e.g.*, $N(C_4H_9)_4BF_4$][8] and, perhaps of more practical interest, from aqueous electrolytes containing 0.1-0.8 M oxalic acid (known for producing a porous oxide layer on aluminum).[9] In this latter case, pretreatment of the aluminum surface by either diamond paste polishing or by anodic activation into the pitting region was an essential step prior to electrodeposition. Even then, at low concentrations of pyrrole (0.1 M), film deposition was patchy and the deposition potential increased during galvanostatic deposition, attributed to growth of an Al_2O_3 layer in parallel with the electropolymerization. Only at high (0.8 M) pyrrole concentration and in the presence of 0.1 M oxalic acid could smooth adherent films be produced. The polymerization was still accompanied by growth in the thickness of the Al_2O_3 layer (Al corrosion), and formation of some overoxidized polypyrrole was noted.[9] Overoxidation increases the localization (*i.e.*, hinders delocalization) of the charge carriers in the polymer, leading to reduced conductivity. It was suggested that overoxidized polypyrrole filled the Al_2O_3 pore structure (a composite dielectric) that was sandwiched between the aluminum substrate and a conducting polypyrrole overlayer.

Recent reports by Lacroix and co-workers describe the electrodeposition of polyaniline on mild steel and zinc.[13,14] Homogeneous, strongly adherent polyaniline films were obtained on mild steel by galvanostatic deposition from neutral aqueous solution in the presence of $LiClO_4$, known to passivate mild steel. The deposition apparently occurred on the passive layer, and an efficiency of 90% was reported.[14] Polyaniline was also deposited on mild steel and on zinc after first depositing a thin (1 μm) film of polypyrrole on the substrate. This two-step process apparently involved very little dissolution of the substrate and the polyaniline appeared to grow on the surface of the polypyrrole.[13] The polypyrrole films were deposited from an aqueous medium containing sodium salicylate and pyrrole.[15] The salicylate was reported to form a passivating, nonblocking layer on a variety of active metals including aluminum, permitting the electropolymerization of pyrrole with a current efficiency close to 100%. However, no data for aluminum was provided.

If oxidation of the monomer (*e.g.*, pyrrole) and/or subsequent formation and deposition of the polymer (*e.g.*, polypyrrole) are kinetically limited at a metal electrode such as Al or one of its alloys, then electron transfer mediation may be useful in reducing the overpotential required for oxidation and deposition, perhaps alleviating

* Electrochemical Society Active Member.
** Electrochemical Society Student Member.
z E-mail: dennis.tallman@ndsu.nodak.edu

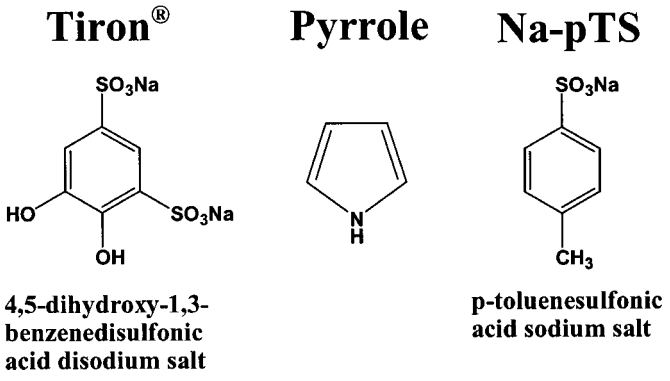

Figure 1. The structures of Tiron (4,5-dihydroxy-1,3-benzenedisulfonic acid disodium salt), pyrrole, and *p*-toluene sulfonic acid sodium salt (Na-*p*TS).

the problems of Al corrosion and polymer overoxidation noted above. Electron transfer mediators, including various aromatic hydrocarbons and heterocycles, have the ability to lower the overpotential of such redox reactions and have been used as catalysts in organic and biological redox reactions.[16-19] Indeed, Tiron (4,5-dihydroxy-1,3-benzenedisulfonic acid disodium salt) has been shown to catalyze the electrodeposition of several conducting polymers (including polypyrrole) on platinum electrodes, reducing the deposition potential by up to 200 mV.[20] To our knowledge, this approach has not been applied to active metals such as aluminum and its alloys. However, it is interesting to note that the electrodeposition of polypyrrole in the presence of salicylate,[15] described in the preceding paragraph, may have involved electron transfer mediation. Indeed, the authors noted that pyrrole was electropolymerized at very low potentials and that the salicylate ion was oxidized at platinum and at active metal electrodes. We observe from their voltammograms that the potential at which salicylate was oxidized corresponds to the potential at which polypyrrole was formed, suggesting that electron transfer mediation may be involved in their electrodeposition. However, these workers did not consider such a mechanism.

In this paper, we describe the use of electron transfer mediation for the direct electrodeposition of polypyrrole from aqueous solution onto aluminum and onto Al 2024-T3 alloy, focusing on the use of Tiron (Fig. 1) as the mediator.[d] In such experiments, Tiron serves as both the mediator and the dopant anion for the ECP. However, we note here that other benzenediols (*e.g.*, catechol) also mediate the electrodeposition, in which case, the functions of mediator and dopant can be separated (results to be published in due course). Furthermore, since Tiron is a complexing agent capable of binding metals ions such as aluminum and copper, it was anticipated that Tiron might also promote adhesion and/or otherwise stabilize the polypyrrole/Al alloy interface. For example, enhanced sensitivity for copper was observed for polypyrrole-based potentiometric sensors doped with Tiron.[21] Thus, the goal of this work was to develop a process for the direct electrodeposition of polypyrrole on Al and its alloys from aqueous solution using a minimum of surface preparation, producing coatings that have improved adhesion (compared to solvent-cast coatings), little or no overoxidation of the polypyrrole, and reduced Al corrosion during deposition.

Polypyrrole depositions were carried out under galvanostatic conditions at current densities of 1 mA/cm^2. The mediator reduced the deposition potential by nearly 500 mV compared to deposition performed in the absence of mediator (where Tiron was replaced by *p*-toluene sulfonic acid sodium salt, *p*TS). Polypyrrole formation and deposition appears to occur with nearly 100% current efficiency and uniform films are obtained. The results of characterization of these films by scanning electron microscopy (SEM), atomic force microscopy (AFM), X-ray photoelectron spectroscopy (XPS), conductivity measurements, and adhesion measurements are presented.

[d] Patent pending.

Experimental

Materials.—Aluminum alloy 2024-T3 was purchased from Q-Panel (Cleveland, OH) and 1.0 mm thick pure aluminum panels (99.99%) were obtained from Alfa Aesar. The metal substrate surface was prepared by polishing with 600 grit SiC paper followed by degreasing with hexane. Pyrrole and sodium *p*-toluene sulfonate (Na-*p*TS, 95%) were purchased from Aldrich and Tiron from Fluka. For the results reported here, the electrodeposition solution contained 0.05 M pyrrole monomer (freshly distilled) and either 0.05 M Tiron or 0.05 M Na-*p*TS. No additional electrolytes were used. Experiments performed with 0.10 M concentrations of the above species gave virtually identical results. The structures of pyrrole, Tiron, and Na-*p*TS are depicted in Fig. 1.

Electrochemical polymerization.—Electrochemical polymerization/deposition was performed in a one-compartment 500 mL three-electrode cell having an aluminum or Al 2024-T3 working electrode, a platinum plate counter electrode, and a Ag/AgCl reference electrode. The working and counter electrodes had similar areas and were arranged parallel to one another to ensure uniform current distribution. The polypyrrole films were electrodeposited using the galvanostatic mode at a current density of 1 mA/cm^2 using an EG&G Princeton Applied Research potentiostat/galvanostat model 273A. All potentials are reported *vs.* the saturated Ag/AgCl reference electrode.

Surface characterization.—Surface morphology and analysis of the electrodeposited polypyrrole films were carried out using a JOEL 6300 JSM SEM equipped with a Noran Vantage energy dispersive X-ray analyzer that includes a digital pulse processor with a SiLi 10 mm^2 crystal. The Norvar window operated at a working distance of 15 mm from sample surface with a 30° take-off angle. SEM images were taken at 15 kV with different spectral resolution ranges.

AFM of the polypyrrole films was performed on 6 mm^2 samples using a Nanoscope IIIa (Digital Instruments). All images were obtained in air under ambient conditions and were collected over a scan range of from 100 μm to 2 μm, depending on the size of the features being imaged.

XPS of the polypyrrole films was performed using a Surface Science Instruments M-Probe XPS spectrometer. The M-Probe utilized a monochromatic aluminum Kα X-ray source (energy ~1486.6 eV) focused on the polypyrrole specimen in an ultrahigh vacuum analytical chamber, typically at 10^{-9} Torr, and photoelectrons in the range of 0 to 1100 eV were detected using a hemispherical analyzer. For this study, all spectral measurements were collected with an analyzer resolution set at 1.5 eV in the fixed transmission mode and atomic percents were determined from measurements of peak areas.

Conductivity measurements.—The electrical conductivity of the as-deposited films was measured using the four-point probe technique (ASTM D 991-89) at ambient conditions with a Signatone S-301. The S-301 standard four-point probe system utilized tungsten carbide tips, a Keithley 220 programmable current source, and a Keithly 2000 digital multimeter. Measurements were performed by sourcing a current of 4.5 mA and measuring the potential across the two inner probes.

Adhesion measurements.—Adhesion measurements of the electrodeposited polypyrrole coatings on the aluminum alloy 2024-T3 were determined by the pull-off strength test according to ASTM standard procedure D-4541-95. The pull-off test was performed by bonding a stud perpendicular to the surface of the polypyrrole film with an epoxy adhesive (Aradite AV100, a two component epoxy paste which was mixed in a 1:1 weight ratio of epoxy to curing agent). The adhesive was cured at ambient temperature for 24 h and

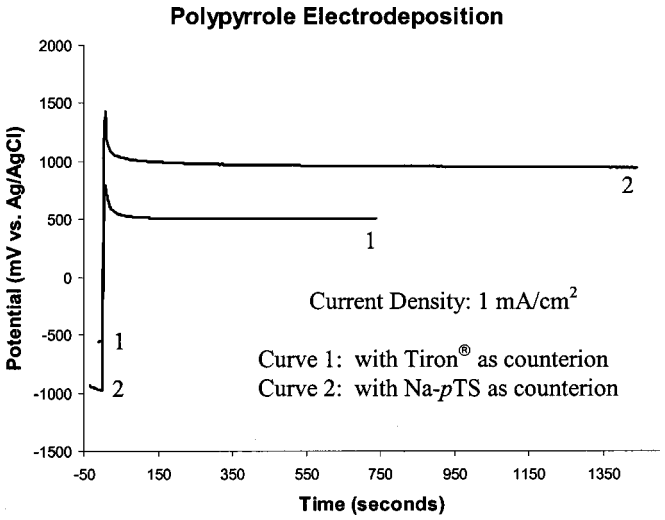

Figure 2. Potential/time curves for the galvanostatic deposition of polypyrrole on Al 2024-T3 at 1 mA/cm^2 current density in the presence of Tiron (curve 1) and in the presence of Na-*p*TS (curve 2).

then transferred to an oven at 40°C for 1 h. The tests were performed using an Elcometer adhesion tester model 106.

Results and Discussion

Electrodeposition studies.—Figure 2 shows potential/time curves for the galvanostatic deposition of polypyrrole (Ppy) at a current density of 1 mA/cm^2 on Al 2024-T3 in the presence of Tiron (curve 1) and, in a separate experiment, in the presence of Na-*p*TS (curve 2). No additional electrolyte was used in these experiments and, therefore, the anion of each salt also served as the counterion (dopant ion) in the deposited polymer. The deposition in the presence of Tiron was terminated at 750 s, at which point a continuous film was obtained (Fig. 3). After an identical 750 s deposition in the presence of Na-*p*TS, the deposited polymer on the alloy surface was very patchy with numerous exposed bare alloy spots. The deposition was continued to the 1440 s mark (Fig. 2, curve 2), at which point an apparently continuous film was obtained (Fig. 3). However, closer inspection by optical microscopy revealed that bare patches of Al alloy remained in the Na-*p*TS polymer film, in spite of the twofold longer deposition time for the Na-*p*TS polymer (Fig 4).

Several additional observations are noteworthy from Fig. 2. The open circuit potential, E_{oc} was recorded for a few seconds prior to application of the current (at time zero). In the presence of 0.05 M Na-*p*TS (curve 2) the E_{oc} was −1.0 V (*vs.* saturated Ag/AgCl), whereas in the presence of 0.05 M Tiron (curve 1) the E_{oc} was *ca.* −0.6 V. Both solutions also contained pyrrole (0.05 M). The Tiron imparted a significantly more noble potential to the aluminum alloy (*ca.* 0.4 V), even before polymer deposition commenced. Once conducting polymer was deposited but with significant exposed bare aluminum still remaining (as at the end of the 1440 s deposition with Na-*p*TS, curve 2, as noted above), the E_{oc} increased to *ca.* −0.2 V. The ECP has the ability to impart a substantial ennobling to the aluminum alloy as noted in previous studies from our laboratory[5] and from elsewhere.[22,23]

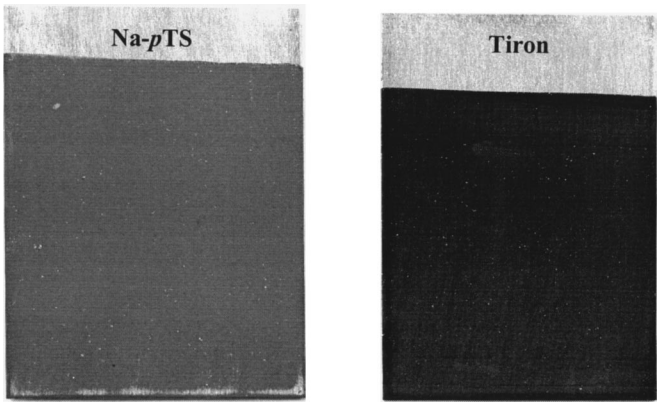

Figure 3. Photographs of polypyrrole films deposited galvanostatically in the presence of Na-*p*TS (1440 s, deposition, left) and Tiron (750 s deposition, right).

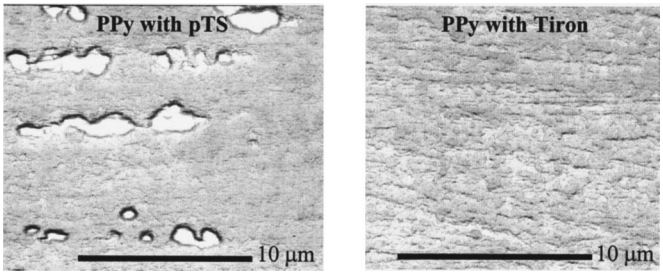

Figure 4. Optical micrographs of polypyrrole films deposited galvanostatically on Al 2024-T4 in the presence of Na-*p*TS (1440 s deposition, left) and Tiron (750 s deposition, right).

The most important revelation from Fig. 2 is that Tiron substantially reduced the potential for Ppy deposition at Al 2024-T3 by nearly 500 mV, from *ca.* 1.0 V (plateau region of curve 2, Fig. 2) to *ca.* 0.5 V (plateau region of curve 1). Clearly, this less positive polymerization potential should minimize complications from Al alloy corrosion and polymer overoxidation. The details of the mechanism of this process are still being investigated, but electron transfer mediation is clearly involved. It is also expected that film deposition occurs by a two-stage nucleation and growth process,[20] and the mediator could facilitate both of these stages. We conjecture that interaction of the Tiron with the aluminum oxide surface and subsequent electron transfer may be facilitated by hydrogen bonding interactions between the adjacent hydroxyl groups of Tiron and the oxide surface. Very similar deposition behavior was observed at pure (99.99%) aluminum substrates, so, the microstructure of the Al 2024-T3 surface[24] does not appear to play a significant role in the deposition process. Scanning electrochemical microscopy has been used to demonstrate electron transfer at defect sites in the native oxide film on pure aluminum (>99.99%).[25] It is possible that the mediator facilitates electron transfer at these defect sites, perhaps making available additional sites for nucleation and subsequent polymer growth. *In situ* electrochemical AFM studies conducted in our laboratory (to be reported elsewhere) revealed a significant increase in the number of nucleation sites in the presence of Tiron, supporting this hypothesis.

We note that both the transient (nucleation) and steady-state (growth) regions of the potential-time curve of Fig. 2 are shifted to lower potential in the presence of Tiron. This observation along with AFM and SEM studies of film morphology (*vide infra*) suggest that Tiron mediates both the nucleation process at the alloy surface and the subsequent growth of the polymer particles (*i.e.*, deposition of polymer on polymer).

Film characterization by AFM and SEM.—Figure 5 provides a comparison of the AFM images for the bare Al 2024-T3 alloy surface (prepared as described earlier), for a solvent-cast poly(3-octyl pyrrole) (POP) film,[6] and for the galvanostatically deposited Ppy/Tiron and Ppy/*p*TS films. The bare alloy displays a surface roughness consistent with a 600 grit polish. The solvent-cast POP film (2-3 μm thick) is quite smooth with a few shallow dimples (30-70 nm deep) scattered about the surface. The Ppy/Tiron film image reflects a rather uniform nodular deposition pattern, similar to that

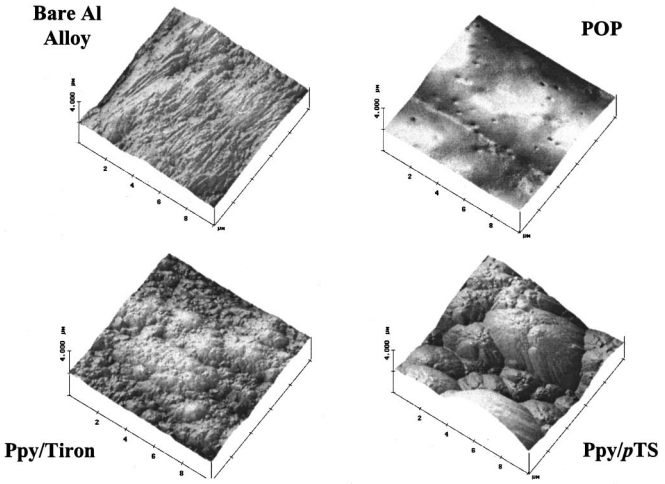

Figure 5. AFMs of (top left) bare Al 2024-T3 alloy and various polypyrrole films deposited on the alloy: (top right) a solvent cast POP film, (bottom left) a polypyrrole film deposited galvanostatically in the presence of Tiron (8 min deposition), (bottom right) a polypyrrole film deposited galvanostatically in the presence of Na-*p*TS (16 min deposition).

observed for polypyrrole with various counterions at platinum electrodes[1,26,27] and an overall surface roughness similar to that of the bare alloy. On the other hand, the Ppy/*p*TS film appears very rough, consistent with a heavily anodized surface and/or large patchy polymer deposition. Thus, Tiron appears to facilitate deposition of polypyrrole on Al 2024-T3 with minimal alteration of the alloy surface.

SEM further illustrates the differences in film growth and subsequent surface morphology between Ppy/Tiron and Ppy/*p*TS. Figure 6 shows films of Ppy/Tiron after 500 and 980 s deposition. At 500 s deposition (top micrograph), the film displayed the nodular surface structure observed by AFM (Fig. 5), with some evidence of roughness on the micrometer scale. By 980 s (bottom micrograph), much of the roughness has been filled in by additional nodular growth, leading to a relatively smooth film surface.

Figure 7 shows SEM micrographs of Ppy/*p*TS films after 980 and 1440 s deposition. In contrast to the Ppy/Tiron film, the Ppy/*p*TS film at 980 s (top micrograph) is quite coarse and continued deposition to 1440 s leads to further growth of a few nodules, resulting in a very coarse deposit (bottom micrograph), consistent with the AFM image in Fig. 5. Between the 980 and 1440 s deposition times, the dimension of polymer nodules approximately tripled. In the absence of the mediator, anodization of the alloy surface and/or polymer overoxidation occurs during electrodeposition (as discussed earlier) and these may be responsible for this film growth behavior. Additionally, as noted in the previous section, Tiron appears to mediate the growth stage of deposition. A comparison of the film structures in Fig. 6 and 7 suggests that this mediated film growth is by additional nucleation and growth of new polymer particles on existing ones, leading to the relatively smooth uniform surface structure observed for the Ppy/Tiron film (Fig. 6).

The cross-sectional views of these films shown in Fig. 8 further illustrate the greater uniformity of the Ppy/Tiron film, both in terms of the compact nodular film structure and overall film thickness. The film thickness measured from such images permits an estimation of current efficiency for polymer deposition, as discussed in a later section.

XPS analysis.—Survey XPS spectra for the Ppy/Tiron and Ppy/*p*TS films are displayed in Fig. 9. Of particular interest are the N (1s) and S (2p) peaks, because the ratio of these peaks provides information about the doping level of each polymer film and, thus, the number of electrons consumed per monomer unit in the film

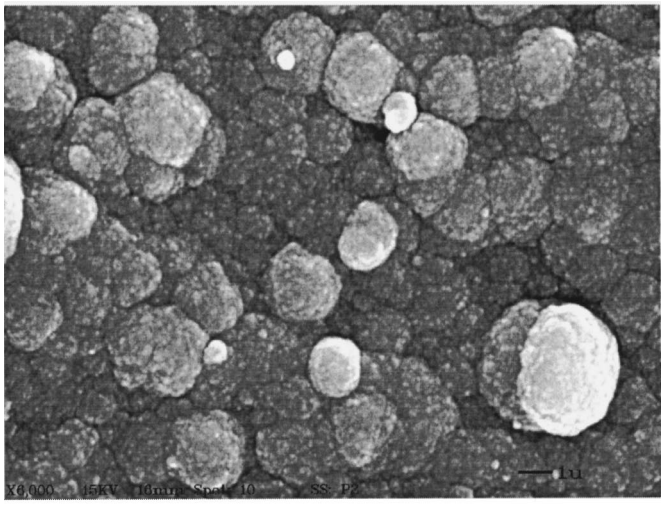

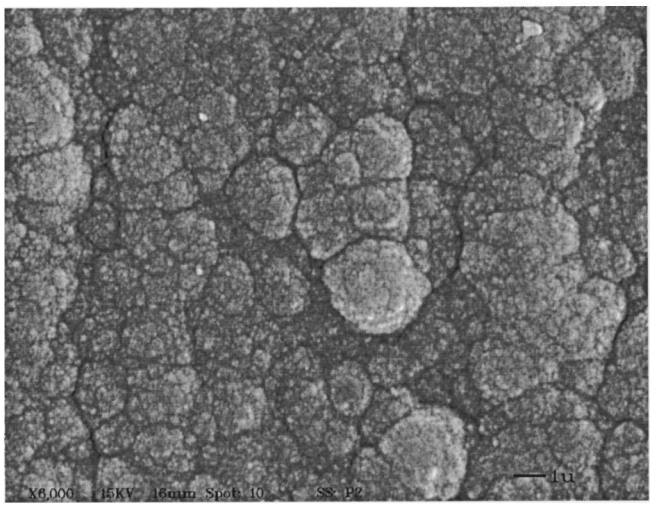

Figure 6. SEM micrographs polypyrrole on Al 2024-T3 deposited in the presence Tiron. (Top image) Deposition at 500 s, (bottom image) deposition at 980 s.

formation. The nitrogen signal arises only from the ring nitrogen of polypyrrole whereas the sulfur signal arises only from the dopant (Fig. 1). From the ratio of the two peak areas, the sulfur-to-nitrogen atom ratio was determined to be 0.366 for the Ppy/Tiron film and 0.318 for the Ppy/*p*TS film (each ratio being an average of measurements on six different films). If we assume that each sulfonate group carries a unit negative charge (*i.e.*, complete ionization of all sulfonate groups), then the doping levels of the two polymer films are similar. Each Tiron anion (with two sulfonate groups) compensates two positive charges on the polymer backbone, whereas each *p*TS anion compensates one positive charge. Thus, half as many Tiron anions would be incorporated into the film as *p*TS anions for a given doping level.

The effective number of electrons transferred per monomer unit during polymer film formation can now be estimated. Two electrons per monomer unit are removed in the polymerization of polypyrrole,[28] with additional electrons removed in the polymer doping process, given by the doping levels computed above. Thus, the apparent n values (n_{app}) are 2.37 for the Ppy/Tiron film and 2.32

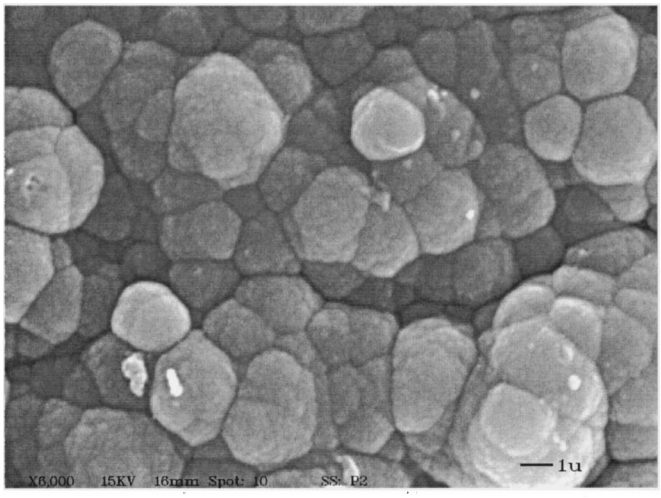

980 s Deposition Time

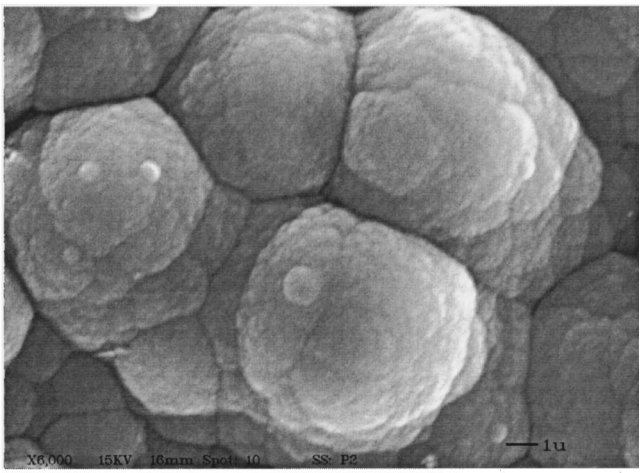

1440 s Deposition Time

Figure 7. SEM micrographs of polypyrrole on Al 2024-T3 deposited in the presence Na-*p*Ts. (Top image) Deposition at 980 s, (bottom image) deposition at 1440 s.

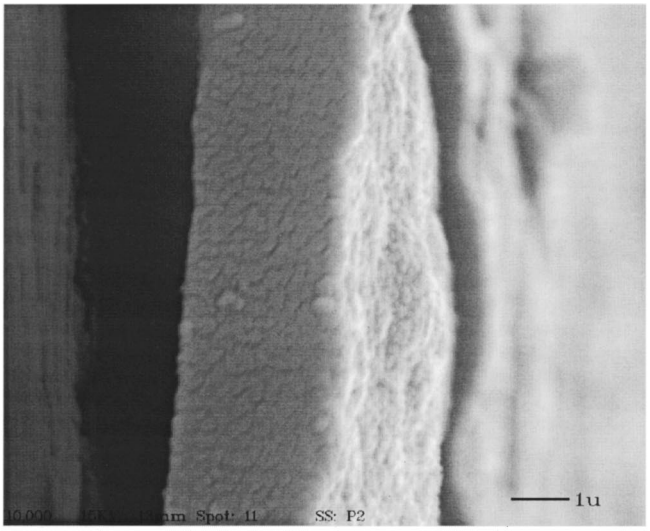

Polypyrrole/Tiron at 980 s Deposition

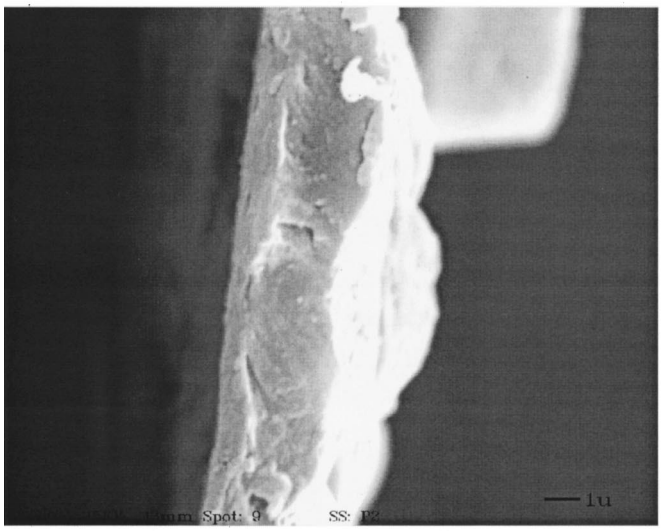

Polypyrrole/*p*TS at 1440 S Deposition

Figure 8. SEM micrographs showing cross-sectional views of electrodeposited polypyrrole on Al 2024-T3. (Top image) Ppy/Tiron at 980 s deposition time, (bottom image) Ppy/*p*TS at 1440 s deposition time.

for the Ppy/*p*TS film. These values compare favorably with previous estimates of 2.25 for polypyrrole.[28] Protons are generated during the polymerization reaction and partial protonation of the sulfonate groups of the Tiron and *p*TS anions would lower the n_{app} values estimated from the XPS data.

Current efficiency.—The current efficiency for polymer deposition can be estimated by comparing the measured film thickness from SEM with that calculated from the total charge consumed. The calculated film thickness δ is given by the expression

$$\delta = \frac{jt}{F} \times EW \times \frac{1}{\rho} \qquad [1]$$

where j is the current density (A/cm^2), t the deposition time (s), F the Faraday constant (C/mol), ρ is the film density (g/cm^3), and EW is the equivalent weight of polymer (g/mol), *i.e.*, mass of polymer deposited per mole of electrons transferred. The EW is obtained by dividing the molar mass of a monomer unit (including associated dopant) by the number of electrons transferred per monomer unit, n_{app}, obtained in the previous section. For Ppy/Tiron, the molar mass is computed as 65.09 g/mol (molar mass of pyrrole minus the two protons displaced during polymerization) plus the mass of Tiron anion associated with each monomer, 0.366/2 of a Tiron anion which equals 49.09 g/mol, for an overall molar mass of 114.18 g/mol. The equivalent weight is then $114.18/n_{app}$, or 48.2 g/mol. Similarly, the equivalent weight of Ppy/*p*TS is 51.5 g/mol.

The density of the deposited Ppy/Tiron film was calculated to be 1.74 g/cm^3 based on mass gain, area, and film thickness measurements for deposited films. This value is somewhat higher than a previously reported value of 1.5 g/cm^3,[29] though the Tiron mediated films prepared in the present work do appear to be very compact and, perhaps, more dense. The density of the Ppy/*p*TS film was not measured, so the literature value of 1.5 g/cm^3 was used.

Film thickness can now be calculated using Eq. 1. For the Ppy/Tiron film of Fig. 8, j was 0.001 A/cm^2 and t was 980 s, with equivalent weight and density provided above. The calculated film thickness is 2.8 μm, which is remarkably close to the measured film thickness of 2.6 μm (from Fig. 8), with both numbers subject to an

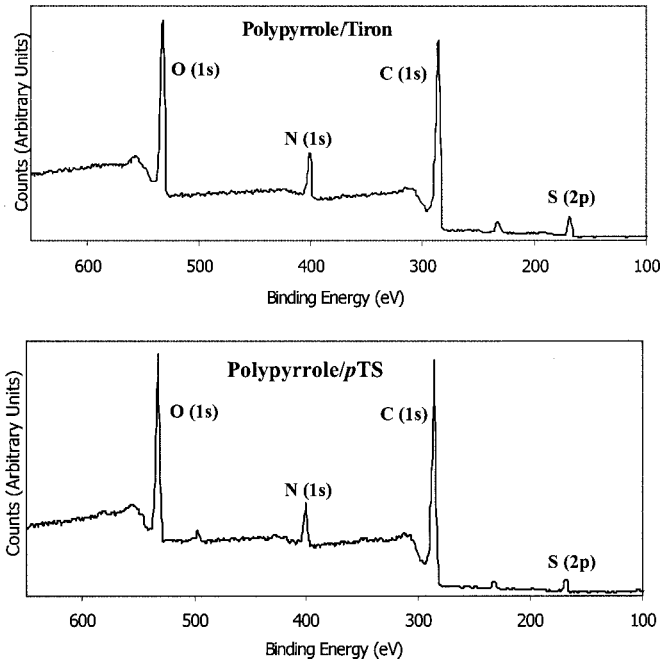

Figure 9. XPS survey spectra for a (top) Ppy/Tiron film, and a (bottom) Ppy/*p*TS film.

estimated uncertainty of at least 10%. This result strongly suggests that nearly 100% current efficiency is achieved in the Tiron-mediated electrodeposition of polypyrrole on the Al alloy. For the Ppy/*p*TS film of Fig. 8, a calculated film thickness of 5.1 μm is obtained, compared with a measured value of *ca.* 3 μm, indicating a current efficiency of *ca.* 60%, although the variation in film thickness (Fig. 8) precludes a good estimate of this value. Nevertheless, it appears that a substantial portion of the current during Ppy/*p*TS deposition is associated with anodic dissolution or passivation of the metal, as suggested by earlier workers.[10]

Conductivity measurements.—Due to excellent adhesion of the Ppy/Tiron films on the Al alloy (*vide infra*), it was not possible to remove the films from the alloy surface for conductivity measurement. Consequently, measurements were made on the as-deposited film using the four-probe technique, recognizing that the values obtained might be higher than those obtained from freestanding films (due to conductivity of the underlying substrate). Nevertheless, a comparison of the relative values of the conductivities is still useful. The measured conductivity for the Ppy/Tiron film was 250 S/m and that for Ppy/*p*TS was 39.5 S/m. The lower value of the conductivity for the Ppy/*p*TS film may reflect an increased thickness of the oxide layer on the underlying alloy, a result of the more positive deposition potential for this film. The lower conductivity could also be due to some overoxidation of the polypyrrole, again a result of the more positive deposition potential. As noted earlier, the doping levels of the Ppy/Tiron and Ppy/*p*TS films determined from XPS are similar. However, XPS measures only the doping level of polypyrrole at the film surface. It is possible that polypyrrole near the alloy interface and/or incorporated into the Al_2O_3 pore structure was overoxidized at the more positive deposition potential of the Ppy/*p*TS film, as suggested in the earlier work of Huelser *et al.*[9] The greater disorder in the Ppy/*p*TS film (evident in Fig. 8) would also likely contribute to a lower conductivity. In any event, the Tiron mediator appears to lead to the formation of more highly conducting polypyrrole films on the Al 2024-T3 substrate.

Adhesion measurements.—Adhesion and cohesion of the ECP film to the metal substrate is an important issue for many applications of ECPs, but particularly for corrosion control applications. Work in our laboratory with organic solvent soluble forms of polypyrrole indicated that modest adhesion could be achieved by a solvent casting approach. For example, a coating of POP having a mixture of perchlorate and *p*TS dopant anions on Al 2024-T3 (the POP film in Fig. 5) exhibited an adhesion of 333 ± 208psi (2.30 ± 1.43 MPa), with failure being primarily cohesive failure.[7]

It was anticipated that direct electrodeposition of a polypyrrole film on the Al alloy would result in improved adhesion and cohesion. Improved adhesion might be anticipated if a large number of nucleation sites on the oxide surface could be realized, providing a large number of attachment points for the polymer film. The electron transfer mediator Tiron appears to lead to an increase in the number of nucleation sites on Al and Al alloy surfaces as discussed earlier. Improved cohesion might be anticipated due to the larger molecular weight achievable by direct electrodeposition compared to solvent casting, where typically only lower molecular weight fractions of the polymer are soluble. Larger molecular weight leads to increased chain entanglement and improved cohesion. Additionally, the Tiron used as mediator and dopant is a well-known metal complexing agent, and might further promote adhesion of the Ppy/Tiron film to the alloy surface.

The Ppy/Tiron film exhibited an adhesion of 887 ± 113 psi (6.12 ± 0.78 MPa), significantly higher than the solvent cast film, and failure was characterized by cohesive failure only. There was no observable adhesive failure at the metal/polymer interface and, thus, adhesion of the Ppy/Tiron film was exceptional. By contrast, the adhesion of the Ppy/*p*TS film was only 53 ± 5 psi (0.37 ± 0.03 MPa), with failure characterized by a mixture of cohesive and adhesive failure. Clearly, Tiron mediated electrodeposition leads to a polypyrrole film with significantly improved adhesion to the Al alloy.

Conclusions

Tiron (4,5-dihydroxy-1,3-benzenedisulfonic acid disodium salt) is an effective catalyst for the electrodeposition of polypyrrole on Al 2024-T3, lowering the deposition potential by nearly 500 mV. As a result, alloy corrosion and polymer overoxidation during deposition are minimized and nearly 100% current efficiency for polymer deposition is achieved. Continuous uniform polypyrrole films can be formed at lower pyrrole concentrations than is possible in the absence of the catalyst. The film formed in the presence of Tiron has higher conductivity and improved adhesion to the alloy. This general approach to ECP deposition on active metals using electron transfer mediation should facilitate the development of many ECP applications, including coatings for corrosion control. Further studies including long-term corrosion experiments on top-coated samples are underway. Additionally, the extension of this approach to other ECPs and to other active metals is underway and results will be reported in due course.

Acknowledgments

This work was supported by the Air Force Office of Scientific Research, grants F49620-96-1-0284, F49620-99-1-0283, and F49620-97-1-0376 (AASERT), North Dakota State University. G.G.W. acknowledges the continued support of the Australian Research Council in the form of a Senior Research Fellowship. The authors would like to express their appreciation to Dr. Xiaofan Yang (Department of Chemistry, North Dakota State University) for her assistance with AFM analysis and to Dr. John T. Grant at the Research Institute, University of Dayton, OH, for his assistance with the X-ray photoelectron spectroscopy analysis. We would also like to thank Scott Payne of the North Dakota State University Electron Microscopy Laboratory for his assistance in obtaining the scanning electron micrographs.

North Dakota State University assisted in meeting the publication costs of this article.

References

1. G. G. Wallace, G. M. Spinks, and P. R. Teasdale, *Conductive Electroactive Polymers, Intelligent Materials Systems*, Technomic Publishing Co., Lancaster, PA (1997).
2. *Handbook of Conducting Polymers*, T. A. Skotheim, R. L. Elsenbaumer, and J. R. Reynolds, Editors, Marcel Dekker, New York (1998).
3. D. E. Tallman, Y. Pae, G. Chen, and G. P. Bierwagen, in *Proceedings of the Annual Technical Conference of the Society of Plastics Engineers*, p. 1234 (1998).
4. D. E. Tallman, Y. Pae, and G. P. Bierwagen, *Corros. Sci.*, **55**, 779 (1999).
5. D. E. Tallman, Y. Pae, and G. P. Bierwagen, *Corros. Sci.*, **56**, 401 (2000).
6. J. He, V. Johnston-Gelling, D. E. Tallman, G. P. Bierwagen, and G. G. Wallace, *J. Electrochem. Soc.*, **147**, 3667 (2000).
7. V. J. Gelling, M. M. Wiest, D. E. Tallman, G. P. Bierwagen, and G. G. Wallace, *Prog. Org. Coat.* **43**, 149 (2001).
8. F. Beck and P. Huelser, *J. Electroanal. Chem. Interfacial Electrochem.*, **280**, 159 (1990).
9. P. Huelser and F. Beck, *J. Appl. Electrochem.* **20**, 596 (1990).
10. F. Beck, P. Huelser, and R. Michaelis, *Bull. Electrochem.*, **8**, 35 (1992).
11. F. Beck, R. Michaelis, F. Schloten, and B. Zinger, *Electrochim. Acta*, **39**, 229 (1994).
12. F. Beck, V. Haase, and M. Schroetz, *AIP Conf. Proc.*, **354**, 115 (1996).
13. J. C. Lacroix, J. L. Camalet, S. Aeiyach, K. I. Chane-Ching, J. Petitjean, E. Chauveau, and P. C. Lacaze, *J. Electroanal. Chem.*, **481**, 76 (2000).
14. T. D. Nguyen, J. L. Camalet, J. C. Lacroix, S. Aeiyach, M. C. Pham, and P. C. Lacaze, *Synth. Met.*, **102**, 1388 (1999).
15. J. Petitjean, S. Aeiyach, J. C. Lacroix, and P. C. Lacaze, *J. Electroanal. Chem.*, **478**, 92 (1999).
16. C. P. Andrieux, J. M. Dumas-Bouchiat, and J. M. Saveant, *J. Electroanal. Chem. Interfacial Electrochem.*, **87**, 39 (1978).
17. C. P. Andrieux, J. M. Dumas-Bouchiat, and J. M. Saveant, *J. Electroanal. Chem. Interfacial Electrochem.*, **87**, 55 (1978).
18. C. P. Andrieux, J. M. Dumas-Bouchiat, and J. M. Saveant, *J. Electroanal. Chem. Interfacial Electrochem.*, **88**, 43 (1978).
19. C. P. Andrieux and J. M. Saveant, *J. Electroanal. Chem. Interfacial Electrochem.*, **93**, 163 (1978).
20. B. Zinger, *J. Electroanal. Chem.*, **244**, 115 (1988).
21. J. Migdalski, T. Blaz, and A. Lewenstam, *Anal. Chim. Acta*, **322**, 141 (1996).
22. D. E. Tallman, G. Spinks, A. Dominis, and G. G. Wallace, *J. Solid State Electrochem.* (2002), In press.
23. G. M. Spinks, A. J. Dominis, G. G. Wallace, and D. E. Tallman, *J. Solid State Electrochem.* (2002), In press.
24. *Aluminum: Properties and Physical Metallurgy*, J. E. Hatch, Editor, American Society for Metals, Metals Park, OH (1984).
25. I. Serebrennikova and H. S. White, *Electrochem. Solid-State Lett.*, **4**, B4 (2001).
26. K. Idla, A. Talo, H. E. M. Niemi, O. Forsen, and S. Ylasaari, *Surf. Interface Anal.*, **25**, 837 (1997).
27. T. Silk, Q. Hong, J. Tamm, and R. G. Compton, *Synth. Met.*, **93**, 59 (1998).
28. A. F. Diaz and J. I. Castillo, *J. Chem. Soc. Chem. Commun.*, **1980**, 397.
29. A. F. Diaz, J. I. Castillo, J. A. Logan, and W.-Y. Lee, *J. Electroanal. Chem.*, **129**, 115 (1981).